BULLETIN OF THE POLISH ACADEMY OF SCIENCES
TECHNICAL SCIENCES, Vol. 66, No. 3, 2018
DOI: 10.24425/123434

Modeling of dynamics of big size $ZnGeP_2$ crystal growth by vertical Bridgman technique

M. PHILIPPOV[1], Y. BABUSHKIN[1], S. EFIMOV[1]*, S. ZAMYATIN[1], V. RUDNICKI[1], A. TROFIMOV[2], and A. GRIBENYUKOV[2]

[1]Tomsk Polytechnic University

[2]Institute of Monitoring of Climatic and Ecological Systems, Siberian Branch of the Russian Academy of Sciences

Abstract. The results of a modelling of big size single crystal $ZnGeP_2$ growth dynamics in the multi-zone thermal installation based on the vertical variant of the Bridgman technique are given. Trustworthiness of the results modeling is achieved by means of creation of the mathematical model taking into account the particularities of the installation as well as the changes in installation work volume during crystallization. Temperature field changes during crystal growth by numerical technique were examined. It is demonstrated that growth container moving has a significant impact on temperature field in work volume and crystallization isotherm local position. Thus, the actual crystal growth rate differs from the nominal velocity of growth container moving. The data received as a result of modelling should be taken into account in new equipment designing, crystallization process control system development and crystal growth experiments planning.

Key words: crystal growth, temperature field, finite elements method, Bridgman technique.

1. Introduction

At present the Bridgman technique works well for many materials including both multiple compounds and materials having complicated processing behavior [1–6]. The demand for scaled actual use of crystals is followed by requirement of reduction of their production cost, that as a rule requires significant increase of crystals geometric dimension. It is particularly topical in case of non-linear optical materials production which efficiency is a superlinear function of optical beam interaction length. In its turn, the crystals dimensions increase leads automatically to the problem of conservation of requirements to their optical quality and uniformity. As a rule, a simple increase of dimensions of thermal installations work volume and growth containers (GC) doesn't lead to the big size single crystal production with nominal quality, but results in pattern physical characteristics deterioration. It can be caused by many physicotechnical reasons, herewith influence power each of them on crystal properties cannot be determined if the problem of provision of given temperature conditions with required accuracy is not solved.

In fact, interconnection between the thermal installation elements reinforces together with increase of working volume dimensions and its filling. Additional complication of thermal flow structure is connected with GC moving in relation to the fixed elements of the thermal installation and corresponding changes of ratio of melt volume to the volume of crystallized part of the material. Therefore, it is impossible to predict dynamics of key factors changes influencing on structural perfection of a growing crystal, such as crystallization front shape as well values of axial crystal growth rate [8] if there are no technical tools for temperature measurement near the crystallization front and calculations used well-developed computational models.

The main objective of research is creation of the mathematical model taking into account geometric and thermal physics particularities of elements of the installation as well as changes in work volume connected with GC moving.

The main objective of research is a modelling of single crystal $ZnGeP_2$ growth dynamics by the Bridgman technique in the multi-zone thermal installation (MTI) for researching of influence of thermal system interaction processes «growth container – thermal installation» in the mechanical movement GC process in the MTI workspace on the growth crystals of big size.

2. Description of multizone thermal installation

The subject of our research is multizone thermal installation for big size $ZnGeP_2$ single crystal growth by vertical Bridgman technique [7] (Fig. 1).

The working volume of the installation represents a cylinder bounded in radial direction by inner surfaces of the ring heating modules. Inside the cylinder a GC (ampoule with a crucible containing a working agent and a seed crystal) and its support (Fig. 2) is disposed.

In accordance with the installation's function its working volume is divided into 3 parts:

- high-temperature zone (M1–M10) designated for keeping working agent in liquid state;
- low-temperature zone (M18–M23) where temperature condition necessary for grown crystal heat removal is maintained;

*e-mail: efimov@tpu.ru

Manuscript submitted 2016-11-21, revised 2017-03-21, initially accepted for publication 2017-04-11, published in June 2018.

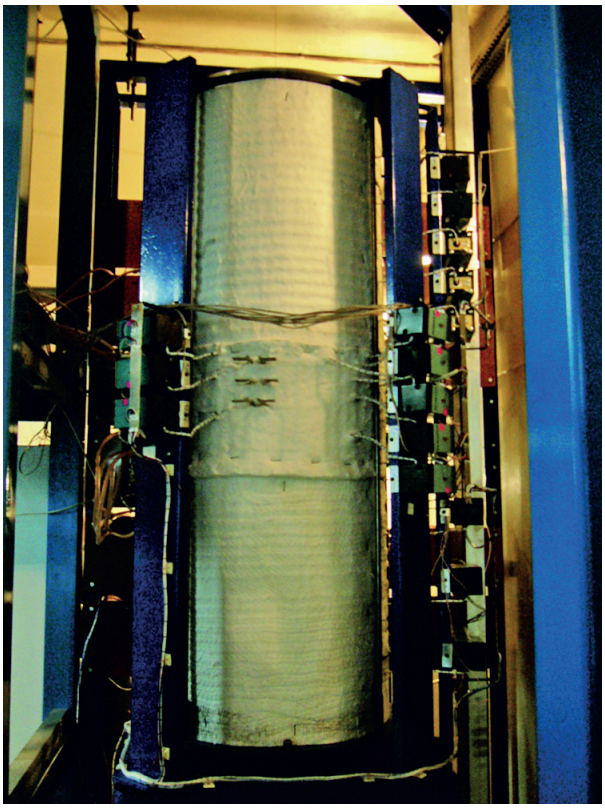

Fig. 1. View of MTI for $ZnGeP_2$ crystal growth by Bridgman technique

- transition zone (M11–M17) where temperature gradient is created and crystal formation takes place.

The main components of MTI are heating modules of various designs. The modules are separated by heat-insulation joints. Resistance elements with different capacity are used to form temperature field (Table 1). Heating modules in transition zone including two heating elements distributed in radius allow us to differentiate their functional designation: the external element with basic energy consumption is supposed to form a high-stable temperature background, and the internal one is designated for precision temperature control in work volume.

During crystal growth the GC with melted working agent inside goes down from high-temperature zone to low-temperature one. Herewith the melt crossing the melting point becomes a crystal. Temperature field control of the installation is carried out by means of distributed PID controller system [9].

Table 1
Maximum heating capacities of heating modules

Heating modules	Q, W
M1, M23	534
M2–M10	197
M11–M17*	52 + 228
M18–M22	325

*Aggregate capacity

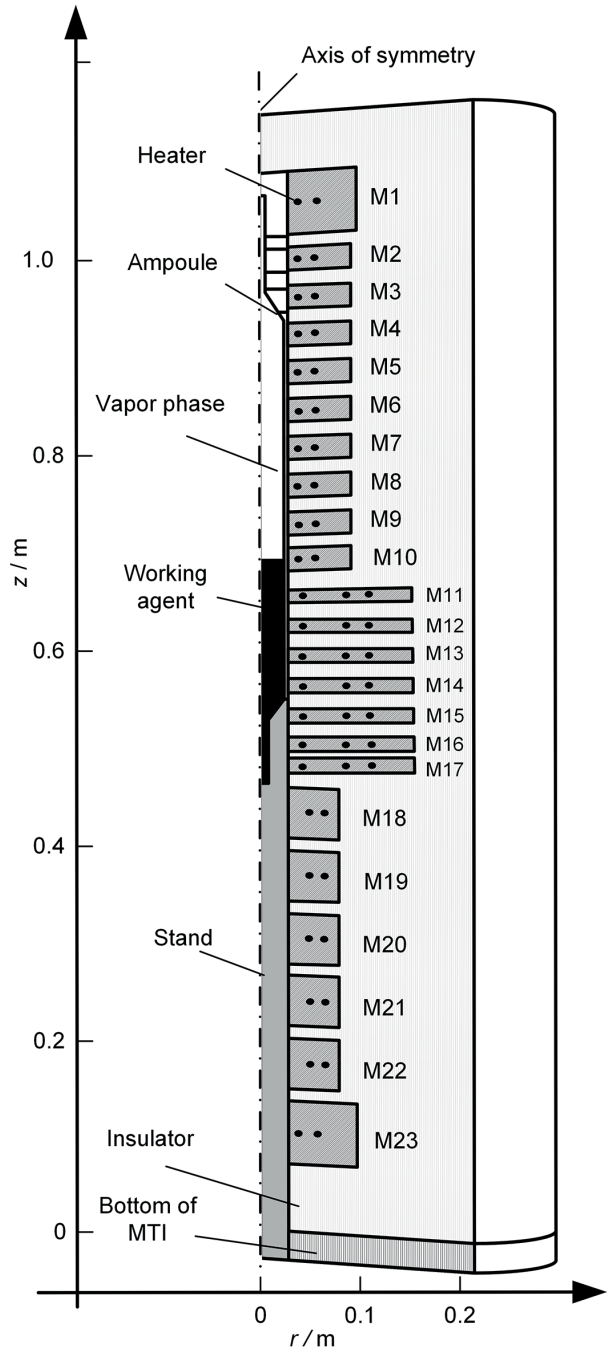

Fig. 2. Scheme of longitudinal sect. of MTI: M1–M23 are heating modules

3. Methods of modeling

The mathematical method is widely used as the most effective approach in search of favorable conditions for crystal growth. Research on modelling may be divided into two groups [10]: modelling of structural defects [11, 12] and modelling of growing process [13, 14]. The first group models describe relationship between conditions for crystal growth and processes of structural defects formation. The models of the second group provide input data for simulations of the first group models,

in particular these models give information about temperature field defining the stress distribution in a growing crystal [15, 16]. The dynamics of crystal growth process is usually simulated as a sequence of quasi-stationary states of the installation temperature field at the GC's different positions [17, 18].

The specific feature of this research is modelling of temperature field in thermally interconnecting system «installation – GC moving inside it». It allows us to study the dynamics of crystal growth process in real-time mode taking in account heat exchange interference of MTI elements with moving GC as well as to receive numerical characteristics of crystal growth which can be closer to real process characteristics.

4. Description of the model

4.1. Mathematical model. Axial symmetry of installation and GC allow us to use the cylindrical coordinate system for numerical calculation, that considerably simplifies the solution of the problem.

Thermal processes in installation and GC can be described as follows:

$$\nabla(k\nabla T) + Q = c\cdot\rho\cdot\partial T/\partial t, \tag{1}$$

where ∇ is Laplace operator; k is thermal conductivity of the material, $W\cdot(m\cdot K)^{-1}$; T is temperature, K; Q is internal heat sources' power (MTI heaters, phase transitions in GC), $W\cdot m^3$; ρ is density, $kg\cdot m^{-3}$; c is specific heat capacity, $J\cdot(kg\cdot K)^{-1}$; t is time, s.

4.1.1. Simplifying assumptions. Position of crystallization front is defined by crystallization isotherm ($T = T_m$, T_m is melting temperature). One can assume that near crystallization front there is a transition layer where thermophysical properties of working agent change from the liquid to solid state.

There are different methods taking into account crystallization heat in Eq. (1). One of them is heat of phase transition's calculation by effective heat $c_{eff} = c + \gamma\Delta H$ implementation [19], where ΔH is latent crystallization heat, γ is Gaussian curve approximating delta-function $\delta(T - T_m)$ and can be defined as $\gamma = \exp\left(-(T - T_m)^2\Delta T^{-2}\right)\left(\Delta T\sqrt{\pi}\right)^{-1}$, [1/K], where ΔT is one-half width of phase transition layer.

The modeling of GC axial movement process relatively installation is performed using the arbitrary Lagrangian–Eulerian method [20–22].

4.2. Boundary conditions. Boundary conditions reflect interaction of MTI with surrounding and heat exchange inside the installation:

1) at the outer boundary of the installation

$$-(k\nabla T) = h\left(T - T_{amb}\right) + \varepsilon\sigma\left(T^4 - T_{amb}^4\right), \tag{2}$$

where h is a heat-exchange coefficient, $W\cdot(m^2\cdot K)^{-1}$; ε is reduced power of emissivity; σ is Stefan-Boltzmann constant, $W\cdot(m^2\cdot K)^{-1}$; T_{amb} is ambient temperature, K;

2) at the inner boundary the matching conditions such as

$$(k_u\nabla T_u) = (k_d\nabla T_d);\ T_u = T_d \tag{3}$$

are used, where indices u and d indicate zones to the left and right of the boundary, correspondingly;

3) heat exchange on the inner surface of installation is given by

$$-(k\nabla T) = \varepsilon_{wv,\,gc}\sigma\left(T_{wv}^4 - T_{gc}^4\right), \tag{4}$$

where indices wv and gc signify surface of the working volume and GC, correspondingly;

4) along the axis r=0 the rotational symmetry condition is used

$$(k\nabla T) = 0. \tag{5}$$

4.3. Moving mesh conditions. Calculation area is divided into two parts:

- area 1 includes MTI and its bottom which remain immobile during the process of crystal growth;
- area 2 including GC, working agent and GC support, moves along axis z

$$dz = -V_{gc}\cdot dt,$$

where V_{gc} is absolute GC moving velocity.

4.4. Initial conditions. During the first start of the model the initial conditions are taken as

$$T = T_{amb} = 293.15\ \text{K}. \tag{6}$$

Subsequent simulation of crystal growth process is carried out with initial conditions based on the results of calculation of MTI stationary temperature field at GC overhead location.

4.5. The solution of the problem. Stationary state of MTI means the temperature change absence, i.e. the condition $\partial T/\partial t = 0$ holds in right part of the expression (1). As this takes place, it is assumed that GC was shut down and crystal growth rate equals zero. In this case it is unnecessary to take special measures for summand $\gamma\Delta H$ nullification during temperatures calculation procedure.

To find the stationary solution of the eq. (1) having zero in right part, the boundary conditions described by (2–5), and initial condition taken from (6) the COMSOL Multiphysics software package [23] based on finite element analysis was used. On the first stage there was built a draft of computation domain reflecting as much as possible all constructional features of both installation and GC. Digitalization of the computation domain was realized on the basis of triangular grid containing 28643 cells. To improve the precision of calculations the grid was additionally thickened up (the maximum size of cell is no more than 1 mm) in the area of working agent location. The boundary conditions, sources of heat generation and thermophysical properties of materials are

given for each MTI elements in (Table 2). The nonstationary problem solution was performed at time spacing equal to 10 min as prescribed.

Table 2.
Thermophysical properties [24–27].

Material	Thermal conductivity k, $W \cdot (m \cdot K)^{-1}$	Density ρ, $kg \cdot m^{-3}$	Heat capacity c, $J \cdot (kg \cdot K)^{-1}$
Material of the heating module	11.5–8.0	2,100.0	1,095.0–1,147.0
Heat insulator	0.333–0.39250	650.0	1,087.0–1,170.0
Heaters	27.7–36.8	7,210.0	780.0–815.0
$ZnGeP_2$	18.0 – crystal 41.4 – melt	4,158.0	392.0 – crystal 682.0 – melt
Work volume/air	0.07	0.31–0.24	1,180.0–1,225.0
GC stand	6.0	2,200.0	1,052.0
Ampoule	1.16–2.32	2,201.0	1,052.0

On the second stage for GC initial position and a seed crystal, correspondingly, there was chosen heat capacity of the heaters, leading to temperature axial distribution nominally providing the process of the $ZnGeP_2$ crystallization – partial melting of seed crystal and complete melting of working agent.

4.6. Tuning parameters of the model. Next stage is a tuning of the developed model parameters on the basis of data to be received in the process of real experiments with the thermal installation described above. Measurements of real axial temperature distribution were made by thermal couple of platinum group Pt-PtRh (10%) with PP(S) calibration using precision device «TERCON» [28]. The thermal couple is kept in a fixed point during 600 s before temperature measurement.

Values of thermal electromotive force go from thermal couple to the input of analog-digital converter of a measuring device, and then into PC for further processing. To receive a more precise value of temperature in the fixed point the set of 60 temperature values measured for the period of one minute is formed. For this set the average value is calculated taken as a true one and used for further calculations.

The procedure of mathematical model parameters tuning was carried out in the following way. In computational scheme the position of GC and height of the area of working agent are set in accordance with real conditions of the experiment. It is assumed that axial temperature distribution in work volume of the installation corresponds to the set of pre-estimated heating capacities of heaters $Q_{1\times30}$. The well-known data from refs. are taken as thermophysical properties which can be considered as initial approximate values. Hereafter, temperature field is calculated.

It is essentially to expect that field estimated at initial approximate values of thermophysical properties will differ from real MTI temperature field. To improve the degree of adequacy of the model to the real object tuning of MTI thermophysical parameters is made. Schematic structure is shown in Fig. 3.

To tune the parameters of the MTI model the sets of values $T^e(z)$ and $T(z)$ in check points are compared in a comparison block. Factor of tuning quality is asymptotically unbiased dispersion of relative deviation of axial temperatures from experimentally measured them in check points of the experimental model

$$err = \left(\sum_{i=1}^{M} \delta_i \right)^{0.5} \cdot \left(M - 1 \right)^{-0.5}, \tag{7}$$

where M is a number of check points, $\delta_i = 2(T_i^e - T_i)^2 (T_i^e + T_i)^{-2}$.

The comparison results (relative root-mean-square dispersion) are entered in the thermophysical properties tuning block.

In this block the model parameter values are corrected by means of their successive (or consecutive) variations. The achievement of the given value of dispersion is the condition for completion of the tuning process.

The number and «denseness» of check points are defined a priori, in relation to character of axial distribution of temperature.

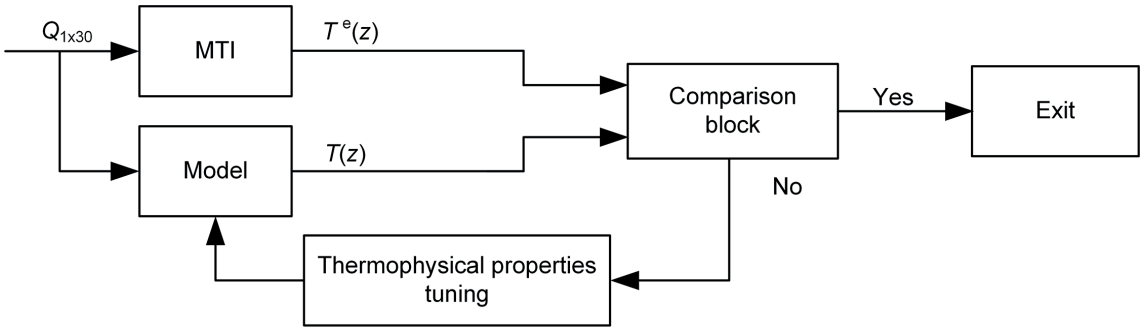

Fig. 3. Scheme of mathematical model thermophysical parameters tuning. $T^e(z)$ and $T(z)$ are temperature axial distributions in work volume of installation and its model

If the condition for completion of the tuning process is not reached, thermophysical parameters of the model should be corrected and the temperature field recalculated. In the process of correction one must control accordance of new set parameters with physically realizable one [7], as well as the correspondence of computational scheme to simulated MTI.

4.7. The results of tuning parameters. The results of tuning parameters of the model are shown in Fig. 4.

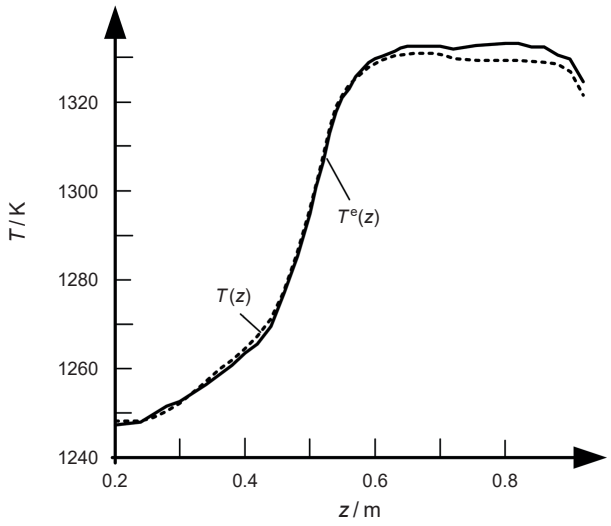

Fig. 4. Axial distribution of temperature

In accordance with achievement of departure of axial temperatures from experimentally measured, not exceeding $\sim$2 K, and dispersion of values $\sim$0.001 (0.1%) calculated on 47 check points, it is concluded that the model parameters are set and it describes the real installation.

5. Computational experiments

Computer simulation of crystal growth process is carried out in the following way. GC geometrical model is set in MTI computational scheme in the position matched with GC position in real installation. Stationary temperature distribution is calculated when heating capacities of heaters in the model are given. Then the non-stationary problem is solved corresponding to GC longitudinal axial movement with a velocity $V_{gc} = 1 \times 10^{-7}$ m $\cdot$ s^{-1} down. Herewith, heating capacities of heaters are adjusted by means of PID controller system. Crystallization border's location, and accordingly latent heat liberation's places, is defined under condition of the equality between melt current temperature and working substance crystallization temperature to a precision of δT: $\left(T(r, z, t) - T_m\right) \leq \delta T$. When the upper boundary of melt goes below crystallization isotherm the simulation is finished. Assuming equality between axial crystal growth rate and mechanical movement velocity of GC the crystal growth continuance is about 491 h.

6. Results and discussion

6.1. The results of stationary model. Numerically calculated distributions of temperature on axis and on work volume surface of MTI are given in Fig. 5.

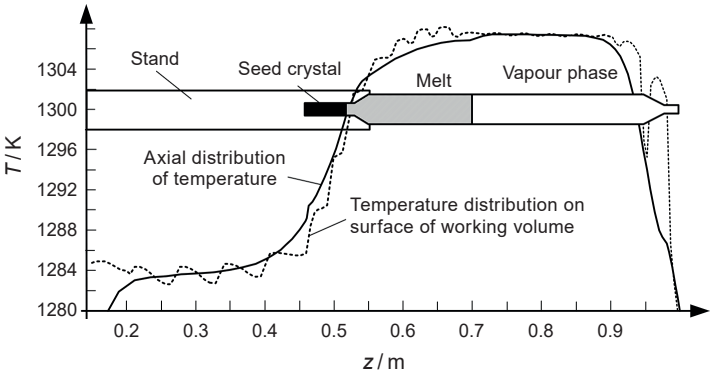

Fig. 5. Temperature distributions in MTI working volume in GC initial position

The analysis of received distributions allows us to distinguish the following characteristics:

- as it was expected, the edge effects result in great drop in temperature on the axis in the upper and the lower parts of work volume of the installation;
- axial distribution of temperature is smooth;
- on the surface of work volume the temperature distribution represents superposition of smooth principal component and wave like excitement associated with spacing of heating modules (M1–M23) separated by heat-insulation joints.

At the beginning of crystal growth simulation the GC lower edge is located at the altitude 0.461 m from lower edge of installation. Herewith the calculated position of the melting point ($T_m = 1300$ K) on the axis of symmetry ($r = 0$) is defined by coordinate $Z^{r=0} = 0.5197$ m, but on the cylinder's surface of the crystal's seed ($r_{seed} = 0.008$ m – radius of the crystal's seed) to coordinate $Z^{r=r_{seed}} = 0.5201$ m. Therefore, at given conditions crystallization isotherm represents concave surface with the radius of curvature $R = r_{seed}^2(\delta Z)^{-1} = 0.16$ m, where $\delta Z = Z_{T_m}^{r=0} - Z_{T_m}^{r=r_{cr}}$ is difference between vertical longitudinal coordinate of crystallization isotherm on the axis of symmetry and on the cylinder's surface of the crystal's seed.

In the general case the concave crystallization front is an unfavorable factor because of possibility of spurious nucleus formation and their overgrowth on periphery of seed crystals.

However, when axial temperature gradient near the crystallization front reaches value equal to (2 K/cm $\rightarrow$ 200 K/m), then supercooling of periphery relatively to the centre of crystal's seed does not exceed 0.1 K, that is comparable with temperature control accuracy in MTI and rather satisfactory for $ZnGeP_2$ single crystal growth.

6.2. The results of simulation of crystal growth. The performed calculations confirm the previous results for the set of

quasistationary models. Calculations (Fig. 6) show that at fixed heating capacities of heating modules, the axial crystal growth rates on the axis $V_z^{r=0}$ and GC periphery $V_z^{r=r_{cr}}$ differ from the value of constant velocity of Vgc movement. Quasi-periodical character of growth rates changes with delay of ~20 h for peripheral growth rate in relation to axial one must lead to the changes of both radius and sign of crystallization front curvature. Such continuous change of crystallization front shape can cause loss of single crystal growth. Crystal growth total time at fixed heating capacities of heating is about 322 h, i.e. about 66% of process duration, which is calculated relying on mechanical motion velocity.

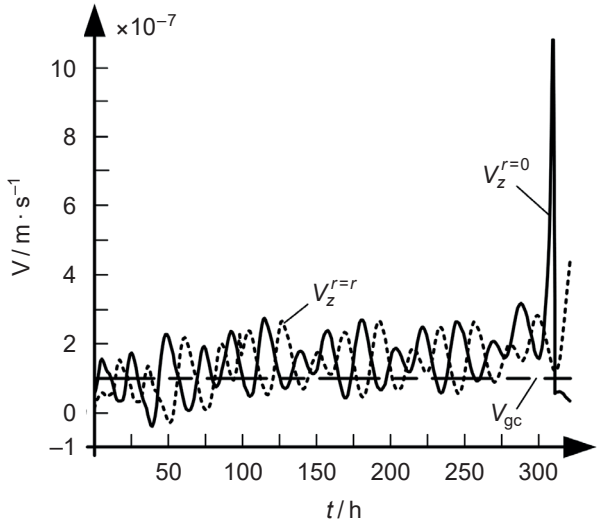

Fig. 6. Change of crystal growth rate in the growth process at fixed capacities of installation heaters

Stabilization of installation temperature field achieved due to control of heaters capacities allows us to control crystallization isotherm and to reduce the amplitude of growth rate variations.

At the beginning of the process ($t <= 48$ h, and length of grown crystal $l_{cr} < 0.066$ m) a form of crystallization front is concave (Fig. 7), thus lower axial crystal growth rate as compared with velocity of GC movement (Fig. 8) gives an advantage for seed crystal overgrowth because in this case a derivation from heat balance condition is reduced.

When conical part of ampoule crosses the crystallization front (t changes from 55 h up to 105 h, 0.068 m $< l_{cr} <$ 0.087 m) the diameter of growing crystal increases from seed crystal diameter to the stationary ampoule diameter, therefore, the problem of suppression of additional crystallization centers formation could become relevant. Fortunately, this problem is blocked out due to higher axial crystal growth rate as compared with its growth rate on periphery of the cone. Moreover, at $t > 49$ h ($l_{cr} > 0.067$ m) curvature of crystallization front changes a sign. So, a concave crystallization front changes into convex. It must contribute in suppression of spurious nuclei crystallization. Form of crystallization isotherm becomes concave only after achievement of

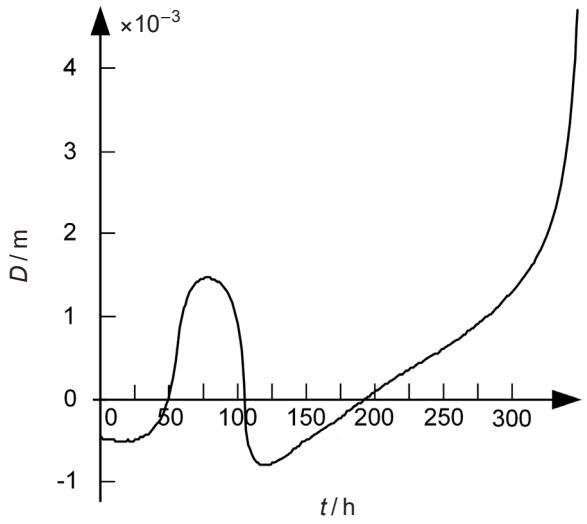

Fig. 7. Change of difference D of crystallization isotherm coordinate on the axis and periphery of growing crystal ($D > 0$ – surface is convex, $D < 0$ – concave)

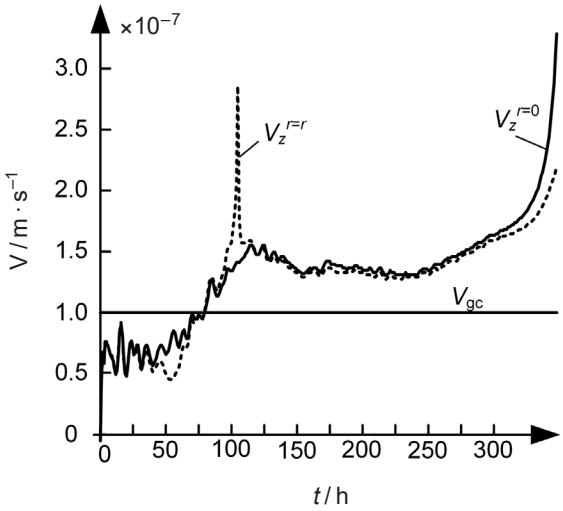

Fig. 8. Change of crystal growth rate in the process of growth at MTI with fixed temperature distribution

the stationary diameter ($t > 105$ h, $l_{cr} > 0.087$ m), but it loses its relevance [1]. Numerical estimates of form of crystallization front correlates well with the results of natural experiments. Fig. 9, 10 present photos of the $ZnGeP_2$ monocrystals longitudinal plate cuts which are grown at stabilization of installation temperature field. On the basis of form of growth striation we may conclude on a form of crystallization front.

In this case the crystal growth rate keeps stable and exceeds the velocity of GC movement in 1.35 times. Increase of crystal growth rate, as a rule, is a disadvantage but a technician having preliminary estimation can choose more workable parameters of processing method. Sharp increase of growth rate on periphery at the moment $t \sim 106$ h ($l_{cr} \sim 0.088$ m) is related to achievement of stationary diameter by a growing crystal (with

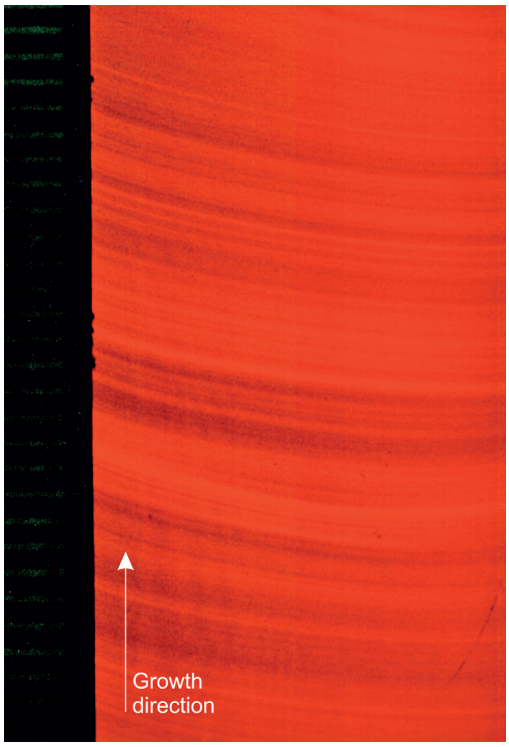

Fig. 9. Photo in transient light for a longitudinal plate cut from the $ZnGeP_2$ single crystal. The plate thickness is 0.5 mm, length along growth axis is 30 mm, diameter is 15 mm. At the left there is a grid ruler

Fig. 10. Photo in transient light for a conical part of thin longitudinal $ZnGeP_2$ slice

GC geometry). The growth rate at the end of the process of crystal growth ($t > 320$ h, $l_{cr} > 0.198$ m) is related to edge effects. Time of crystal growth is $\sim$354 h.

7. Conclusion

The results of modelling the temperature field in work volume of thermal installation with regard to GC movement show that during $ZnGeP_2$ crystal growth by Bridgman technique in thermally interconnecting system, the following is expected:

- in work volume of installation concave crystallization front is initially formed. To reduce probable overgrowth of periphery spurious nucleus differing from seed crystals in orientation and prevent probable loss of single crystal growth, at the initial stage of seed crystal growth it is essential to use minimum velocity of power movement;
- model estimations show that real-time crystal growth rate is not constant and differs from velocity of GC power movement. Their ratio can reach two times at fixed capacities of heaters and will not exceed 35% at stabilization of heaters temperature;
- actual time of crystal growth can differ significantly from nominally determined by velocity GC movement;
- for correction of the form of crystallization front and provision of constant crystal growth rate within all the process of its growth it is necessary to develop control system taking in consideration dynamic change of axial distribution of temperature in installation according to GC position;
- as dynamics of growth rate change on the axis of installation keeps ahead dynamics of growth rate on periphery at fixed capacities of installation heaters, we may conclude that movement of crystallization front is first of all defined by heat energy sink.

References

[1] G.A. Verozubova, A.O. Okunev, A.I. Gribenyukov, A.Yu. Trofimiv, and E.M. Trukhanov, "Growth and defect structure of $ZnGeP_2$ crystals", *J. Cryst. Growth* 312, 1122 (2010).

[2] L. Shen, B. Wang, D. Wu, and Z. Jiao, "Growth of low etch pit density $ZnGeP_2$ crystals by the modified vertical Bridgman method", *J. Cryst. Growth* 383, 79 (2013).

[3] X. Zhao, Sh. Zhu, B. Zhao, B. Chen, Zh. He, R. Wang, H. Yang, Y. Sun, and J. Cheng, "Growth and characterization of the $ZnGeP_2$ single crystals by the modified vertical Bridgman method", *J. Cryst. Growth* 311, 190 (2008).

[4] G. Zhang, X. Tao, Sh. Wang, G. Liu, Q. Shi, and M. Jiang, "Growth and thermal annealing effect on infrared transmittance of the $ZnGeP_2$ single crystal", *J. Cryst. Growth* 318, 717 (2011).

[5] J. Cheng, Sh. Zhu, B. Zhao, B. Chen, Zh. He, Q. Fan, and T. Xu, "Synthesis and growth of $ZnGeP_2$ crystals: Prevention of non-stoichiometry", *J. Cryst. Growth* 362, 125 (2013).

[6] Sh. Xia, M. Wang, Ch. Yang, Z. Lei, G. Zhu, and B. Yao, "Vertical Bridgman growth and characterization of large $ZnGeP_2$ single crystals" , *J. Cryst. Growth* 314, 306 (2011).

[7] M.M. Philippov, A.I. Gribenyukov, V.E. Ginsar, and Yu.V. Babushkin, "Improvement of spatial homogeneity of the $ZnGeP_2$ single crystal growth by the Bridgman method in a vertical geometry", *Russian Phys. J.* 55, 759 (2012).

[8] R.G. Seidensticker, W.R. Rosch, R. Mazelsky, R.H. Hopkins, N.B. Singh, S.R. Coriell, W.M.B. Duval, and C. Batur, "Active control of interface shape during the crystal growth of lead bromide", *J. Cryst. Growth* 198, 988 (1999).

[9] M.M. Philippov, A.I. Gribenyukov, and Yu.V. Babushkin, "Sistema upravlenia technologichesich processov vyrashivania kristallov metodom Bridzhmana", *Sensors and systems* 6, 2 (2012) (in Russian).
[10] G. Muller and J. Friedrich, "Challenges in modeling of bulk crystal growth", *J. Cryst. Growth* 266, 1 (2004).
[11] M.A. Zaeem, H. Yin, and S.D. Felicelli, "Comparison of cellular automation and phase field models to simulate dendrite growth in hexagonal crystals", *J. Mater. Sci. Technol.* 28, 137 (2012).
[12] G.M. Owolab and H.A. Whitworth, "Modeling and simulation of microstructurally small crack formation and growth in notched nickel-base superalloy component", *J. Mater. Sci. Technol.* 30, 203 (2014). http://dx.doi.org/10.1016/j.jmst.2013.09.011.
[13] N. Song, Y. Luan, Y. Bai, Z.A. Xu, X. Kang, and D. Li, "Numerical simulation of solidification of work roll in centrifugal casting process", *J. Mater. Sci. Technol*. 28, 147 (2012).
[14] J. Amon, P. Berwian, and G. Muller, "Computer-assisted growth of low-EPD GaAs with 3'' diameter by the vertical gradient-freeze technique", *J. Cryst. Growth* 198, 361 (1999).
[15] H. Ouyang and W. Shyy, "Numerical simulation of CdTe vertical Bridgman growth", *J. Cryst. Growth* 173, 352 (1997).
[16] W.R. Rosch, A.L. Fripp, W.J. Debnam, and T.K. Pendergrass, "Performance testing of a vertical Bridgman furnace using experiments and numerical modeling", *J. Cryst. Growth* 174, 139 (1997).
[17] M. Metzger, "Optimal control of crystal growth processes", *J. Crystal Growth* 230, 210 (2001).
[18] A. Yeckel, G. Compere, A. Pandy, and J.J. Derby, "Three-dimensional imperfections in a model vertical Bridgman growth system for cadmium zinc telluride", *J. Cryst. Growth* 263, 629 (2004).
[19] C. Bonacina, G. Comini, A. Fasano, and M. Primicerio, "Numerical solution of phase-change problems", *International J. of Heat and Mass Transfer* 16, 1825 (1973).
[20] E. Kuhl, H. Askes, and P. Steinmann, "An ALE formulation based on spatial and material settings of continuum mechanics. Part 1: Generic hyperelastic formulation", *Computer Methods in Appl. Mechanics and Engineering* 193, 4207 (2004). http://dx.doi.org/10.1016/j.cma.2003.09.030.
[21] R. Boman and J.-P. Ponthot, "Enhanced ALE data transfer strategy for explicit and implicit thermomechanical simulations of highspeed processes", *International j. of Impact Engineering* 53, 62 (2013). http://dx.doi.org/10.1016/j.ijimpeng.2012.08.007.
[22] L. Braescu and T. F. George, "Arbitrary Lagrangian-Eulerian method for coupled Navier-Stokes and convection-diffusion equations with moving boundaries", *Proceedings of the 12th WSEAS Int. Conf. on Appl. Mathematics*, pp. 31–37, Part 1, Egypt, Cairo, 2007.
[23] COMSOL Multiphysics, (http://www.comsol.com, accessed 2014.12. 01).
[24] R.K. Willardson and H.L. Goering, *Compound Semiconductors* (Reinhold, New York, 1966).
[25] A.D. Sventchanskiy, *Elektricheskie promyshlennye pechi* [*Electrical industrial furnaces*] (Moskow, Energiya, 1975) (in Russian).
[26] B.V. Molotilov, *Precizionnie splavi* [*Precision alloys*] (Metallurgiya, Moskow, 1983) (in Russian).
[27] D.N. Nikogosyan, *Nonlinear Optical Crystals: A Complete Survey* (Springer, N.Y., 2005).
[28] TERMEX. (http://www.termexlab.ru accessed 2014.12.01).